Abstract

This paper outlines the process of designing a fiber feed to achieve a stable polarization for use in a polarizing interferometer. It provides a description of the ILIAD Interferometer developed by the Inverse Square Law Group at the University of Birmingham, UK. It investigates the polarization of light and the use of fiber optics while trying to obtain a stable polarization for light passing through an optical fiber. Results of attempts to input light from a fiber feed into the ILIAD interferometer are also presented.

Design Considerations of a Fiber Feed for a Cryogenic Polarizing Interferometer

Jonathan Cripe

August 2, 2011

1 Introduction

1.1 Experiment Overview

Since the early days of science, there has always been a great interest in gravity and how it works. From Newton's gravitational laws to Einstein's general relativity, gravity has been a widely studied aspect of physics. Today, the interest continues as physicists continue to ask how gravity works. Recently, there has been an interest in studying the inverse square law of gravity on distance scales of less than 1 mm. The recent interest has come partly from string theory's predictions of extra dimensions in the universe. It has been proposed that the gravity's inverse square law might break down at small distances because it is diluted in the extra spatial dimensions while the other fundamental forces are constrained to only the three spacial dimensions we are familiar with. According to a recent theory, the real strength of gravity would only be seen if the extra dimensions are viewed at very small scales [1]. If this is true, it would violate Newton's inverse square law of gravity.

1.2 ILIAD Interferometer

To test these predictions, the Inverse Square Law Group at the University of Birmingham, UK is developing an experiment with a superconducting

*C. C. Speake, M. J. Nelson

torsion balance. Measuring the displacement of the torsion balance allows the gravitational force to be measured between two masses that are $15\mu m$ apart. An interferometer (ILIAD) is used to measure the changes in displacement of the torsion balance. A picture of the ILIAD interferometer is shown below in Figure 1 and a diagram of the optical components in Figure 2 [2].

The light enters the interferometer by an optical fiber and collimated by a collimator (neither of which are shown) [2]. The first component that the light encounters is polarizing beam splitter A. The light whose electric field is parallel to the plane of incidence is transmitted and lost (not shown in the diagram), and the light whose electric field is perpendicular to the same plane is reflected into the rest of the interferometer. The next element in the path is beam splitter B. The reflected beam is lost (not shown) and the transmitted one propagates further into the following components. The next two optical elements divide the light into the arms of the interferometer. Polarizing beam splitter C reflects the light, whose electric field is oriented at -45° with respect to the preceding polarizers, into one of the arms, and transmits the remaining light whose field is at $+45^\circ$ onto polarizing beam splitter D. The latter component reflects the whole remaining beam into the second arm and ideally no light is transmitted.

The following components that lie along the arms are the ones responsible of folding the beams onto the mirrors whose movement the whole device aims to sense. Figure 3 [2] shows a diagram of one of these assemblies. In both arms the polarization directions of the light are perpendicular to their respective planes of incidence at polarizing beam splitters E and E', and ideally the two beams are completely reflected and no component of the light is transmitted. In the diagram shown, after the reflection the light then goes through quarter-wave plate F. The fast axis of the plate is oriented at 45° with respect to the plane of incidence at E, thus changing the linear polarization to circular polarization. The light reaches the target mirror G. The reflection produces a misalignment in the propagation direction of the beam twice as large as the actual tilt of the mirror. The light is reflected back to quarter-wave plate F. The polarization changes back to linear and its direction is now perpendicular to the polarization direction it had when it was first reflected by polarizing beam splitter E. Therefore, the light now goes through the splitter rather than being reflected. The light then reaches the cat's eye retroreflector, which comprises the lens H and the mirror I, and is reflected back in the direction from which it came. The ray goes through beam splitter E again, and the light becomes circularly polarized by going

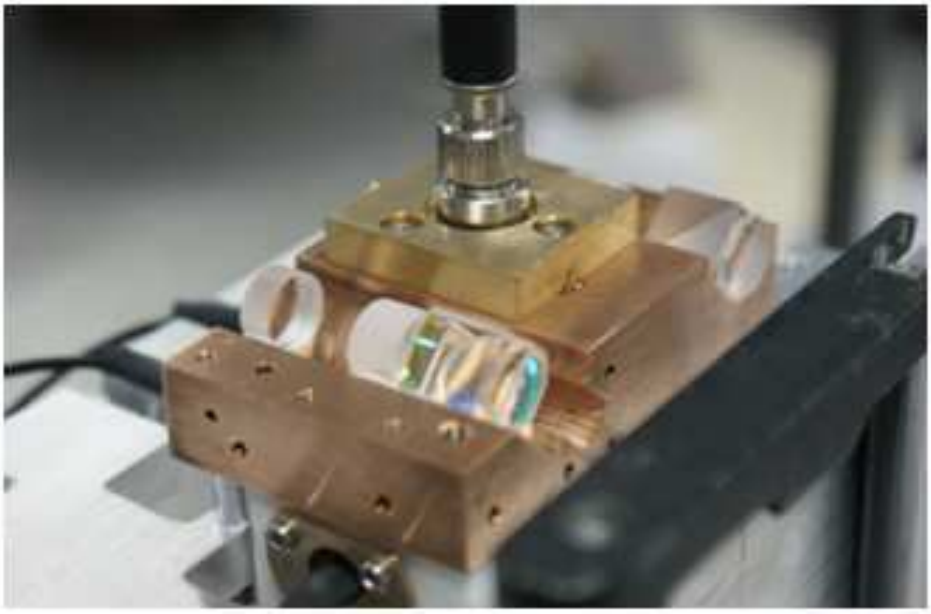

Figure 1: ILIAD Interferometer

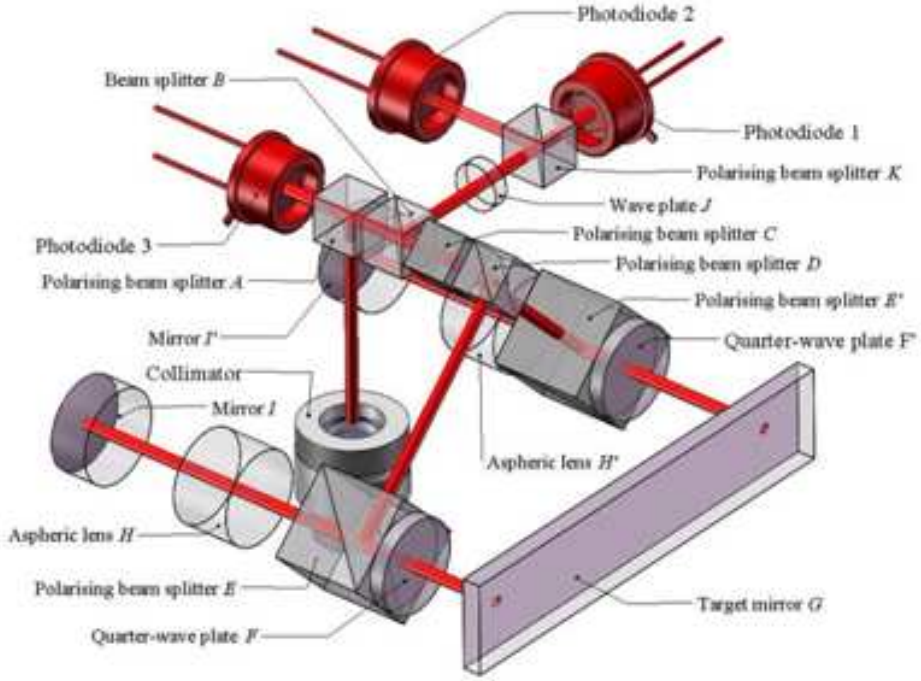

Figure 2: ILIAD Interferometer Diagram

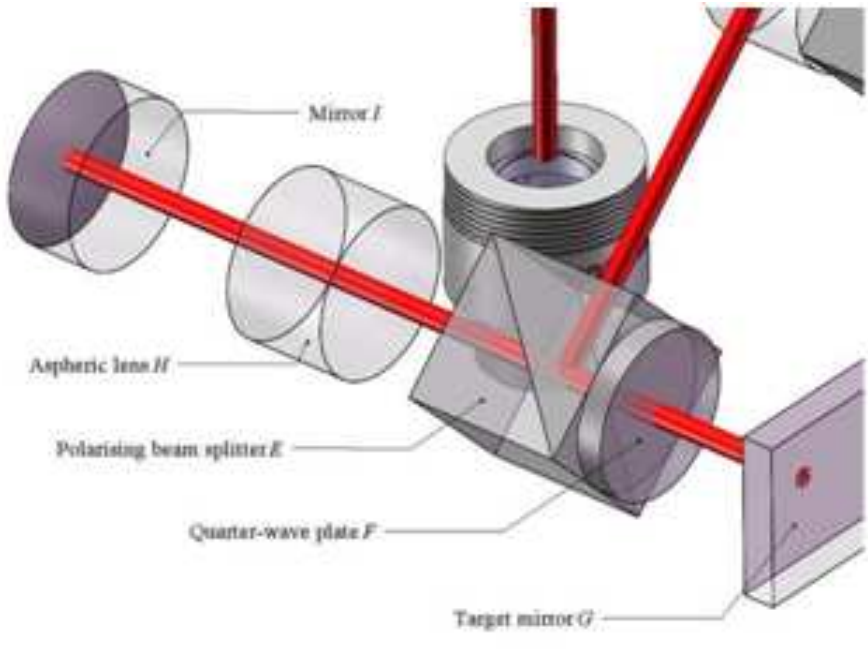

Figure 3: Diagram of one arm of the ILIAD Interferometer

through quarter-wave plate F. The beam encounters the tilted mirror G for a second time and is not translated with respect to the beam. This reflection yields a beam parallel to the original incident beam on the mirror. The light propagates back to quarter-wave plate F, changing its polarization back to linear, but this time its direction is perpendicular to the plane of incidence at polarizing beam splitter E. The light is thus reflected by E propagating back to polarizing beam splitter D, from which it is further reflected into the rest of the interferometer. The description of the path that the light follows along the other arm is analogous.

As shown in Figure 2, both beams recombine at polarizing beam splitter C and subsequently propagate onto the set of components responsible for producing the interference patterns. The beam splitter B divides the light into two beams. The transmitted beam reaches polarizing beam splitter A, where the interference pattern, whose intensity is measured by photodiode 1, is created upon transmission. The reflected beam at beam splitter B

goes through quarter-wave plate J and then two interference patterns are created upon reflection and transmission at polarizing beam splitter K. The intensities of those patterns are measured by photodiodes 2 and 3.

1.3 Motivation

As described above, the light going into the interferometer needs to be polarized when it enters the interferometer. In addition, the polarization needs to be constant to reduce noise in the interferometer output. Previous attempts to achieve a constant polarization were unsuccessful and contributed to a substantial amount of noise in measurements. My goal was to determine a reliable, repeatable method of getting a constant polarization orientation out of the fiber to be put into the interferometer.

1.4 Polarization and Stokes Parameters

In 1852, George Gabriel Stokes characterized the polarization state of light in terms of four intensity parameters now known as the Stokes polarization parameters. The Stokes parameters are frequently used to describe the polarization of light by relating the parameters to the polarization ellipse [3].

The polarization of light can be described as the orientation of the wave's electric field over the period of an oscillation. If the optical beam is traveling in the z direction, then the orthogonal components of the electric field can be described as

$$E_x(z,t) = E_{0x}\cos(\omega t - \kappa z + \delta_x) \tag{1.1}$$

$$E_y(z,t) = E_{0y}\cos(\omega t - \kappa z + \delta_y) \tag{1.2}$$

where t represents time, E_{0x} and E_{0y} are the maximum amplitudes of the optical field, $\omega = 2\pi\nu$ is the angular frequency, $\kappa = \frac{2\pi}{\lambda}$ is the wave number, δ_x and δ_y are phase constants, and $\omega t - \kappa z$ describes the propagation of the wave. The polarization ellipse for 100 % polarized (shown in Figure 4) [4] is often used as a visual representation of the field and is described by

$$\frac{E_x^2(z,t)}{E_{0x}^2} + \frac{E_y^2(z,t)}{E_{0y}^2} - \frac{2E_x(z,t)E_y(z,t)}{E_{0x}E_{0y}}\cos\delta = \sin^2\delta \tag{1.3}$$

where $\delta = \delta_y - \delta_x$. Since the ellipse in Eq. 1.3 cannot be observed or measured, Eq. 1.3 must be converted to an intensity, which can be measured, by taking a time average of Eq. 1.3. The time average is

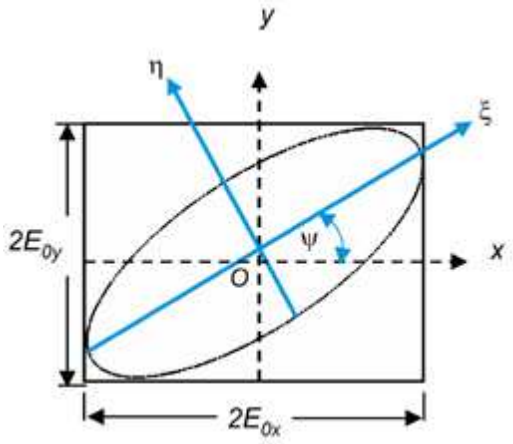

Figure 4: Plot of polarization ellipse, 1.3 , rotated through an angle ψ to a new set of axes (ξ, η).

$$\langle E_i(z,t)E_j(z,t)\rangle = \lim_{T\to\infty}\frac{1}{T}\int_0^\infty E_i(z,t)E_j(z,t)\,\mathrm{d}t \tag{1.4}$$

and produces

$$S_0^2 = S_1^2 + S_2^2 + S_3^2 \tag{1.5}$$

$$S_0 = E_{0x}^2 + E_{0y}^2 \tag{1.6}$$

$$S_1 = E_{0x}^2 - E_{0y}^2 \tag{1.7}$$

$$S_2 = 2E_{0x}E_{0y}\cos\delta \tag{1.8}$$

$$S_2 = 2E_{0x}E_{0y}\sin\delta \tag{1.9}$$

The first parameter, S0, represents the total intensity of the light. S1, S2, and S3 describe the degree of linear polarization (or vertical), linear $+45\,^\circ$ (or $-45\,^\circ$) polarization, and right (or left) circular polarization, respectively. They are often written as the elements of a 4x1 matrix, called the Stokes vector, as

$$\begin{pmatrix} S_0 \\ S_1 \\ S_2 \\ S_3 \end{pmatrix} \tag{1.10}$$

which is normalized by dividing through by S_0. The Stokes parameters also describe partially polarized and unpolarized light as well as the degree of polarization P defined as

$$P = \frac{\sqrt{S_1 + S_2 + S_3}}{S_0} \tag{1.11}$$

1.5 Fiber Optics

Optical fiber consists of a core and a cladding material that has a lower index of refraction. The light that enters the fiber is kept in the core by total internal reflection, allowing the light to travel long distances through the fiber without leaking out. Fibers that support many propagation paths or transverse modes are called multi-mode fibers (MMF), while those that only support a single mode are called single-mode fibers (SMF). The core diameter also determines the wavelengths that are able to pass through the fiber. A connector is attached on both the input and output ends of the fiber to secure it to the mount. The two types of connectors are FC/PC (ferrel connector, physical contact) and FC/APC (ferrel connector, angled physical contact).

In addition, different types of fibers control the polarization of the light in different ways. Polarization maintaining (PM) fibers keep the polarization constant as the light passes through the fiber while non-polarization maintaining fibers do not and allow the light to depolarize. To achieve the stable polarization, PM fibers are constructed from highly birefringent materials that are produced with large stresses [5, 6]. This high amount of stress allows one of the polarization modes to be more strongly guided than the other. The differential radiation loss permits the weakly guided polarization to leak out of the fiber while keeping the strongly guided polarization inside the fiber. To enhance the effect, fibers are bent or coiled to increase the differential radiation loss or polarization-extinction ratio. This ratio is dependent on the type of fiber, the radius of the bend, the number of bends or coils, and the wavelength of light. It is important to note, however, that bending the fiber also produces a transfer of power between polarization modes and produces mechanical stresses on the fiber jacket which can be translated to the connections. Two types of fibers, bow-tie and PANDA, utilize a cross-sectional geometry to maximize the birefringence.

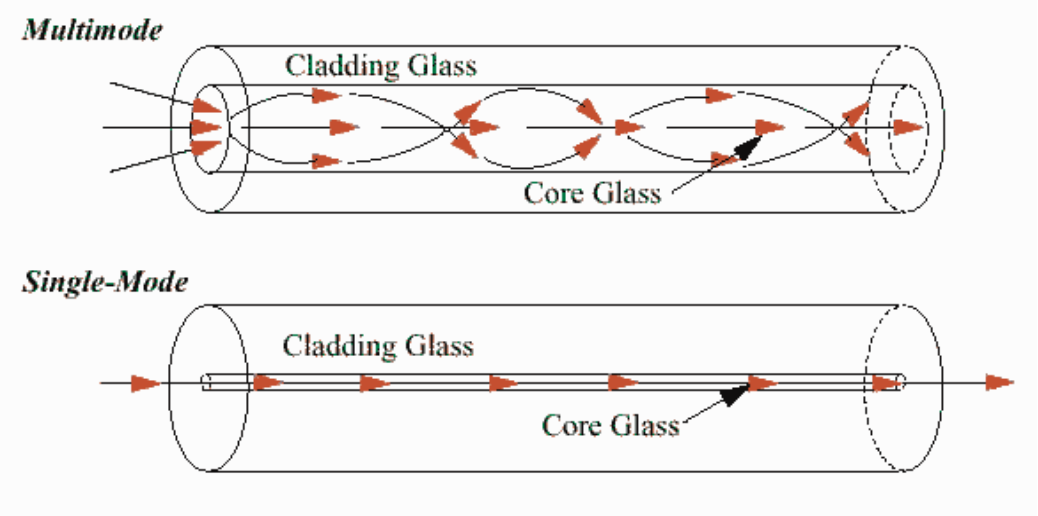

Figure 5: Comparison of SMF and MMF [7]

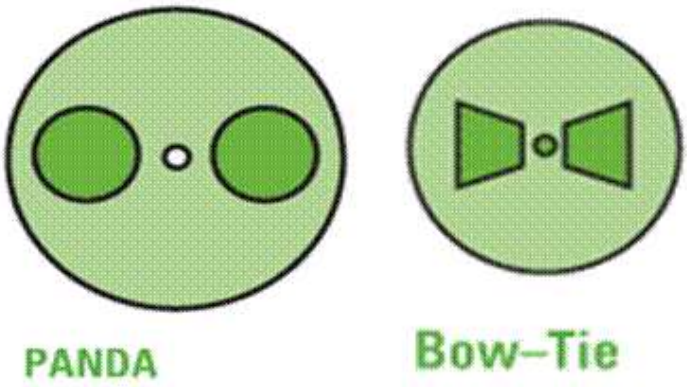

Figure 6: Comparison of PANDA and bowtie PM fibers [8]

2 Measuring Stokes Polarization Parameters

As stated above, the Stokes Polarization Parameters provide a method of describing the polarization of an optical beam. To measure the parameters, we used two different methods. The first method utilizes a single circular polarizer constructed of a quarter wave plate and a polarizer whose transmission axis is at $+45\,^\circ$ with respect to the horizontal x-axis [9]. This method allows the measurement of all four Stokes parameters by allowing the beam to pass through one side of the polarizer and then flipping it around. By only using one optical element, this eliminates the problem with the classical measurement where the optical path density changes by adding and removing optical elements. When the beam passes through the polarizer from the circular side (with the linear polarizer facing the source) the measured intensity is

$$I_c(\alpha) = \frac{1}{2}(S_0 - S_1 \sin 2\alpha + S_2 \cos 2\alpha) \tag{2.1}$$

where α is the angle by which the polarizer is rotated. When the beam passes through the polarizer from the linear side (quarter wave plate facing the source) the measured intensity is

$$I_l(\alpha) = \frac{1}{2}(S_0 + S_3). \tag{2.2}$$

By rotating the polarizer with the circular side facing the source to $0\,^\circ$, $45\,^\circ$, and $90\,^\circ$, and then flipping the polarizer to the linear side and taking measurement at $0\,^\circ$, the Stokes parameters can be derived as

$$S_0 = I_c(0) + I_c(90) \tag{2.3}$$

$$S_1 = S_0 - 2I_c(45) \tag{2.4}$$

$$S_2 = I_c(0) - I_c(90) \tag{2.5}$$

$$S_3 = -S_0 + 2I_l(0). \tag{2.6}$$

A second method of measuring the Stokes parameters uses a rotating quarter wave plate and fixed linear polarizer whose transmission axis is the x-axis [3]. The intensity of the beam that passes through is

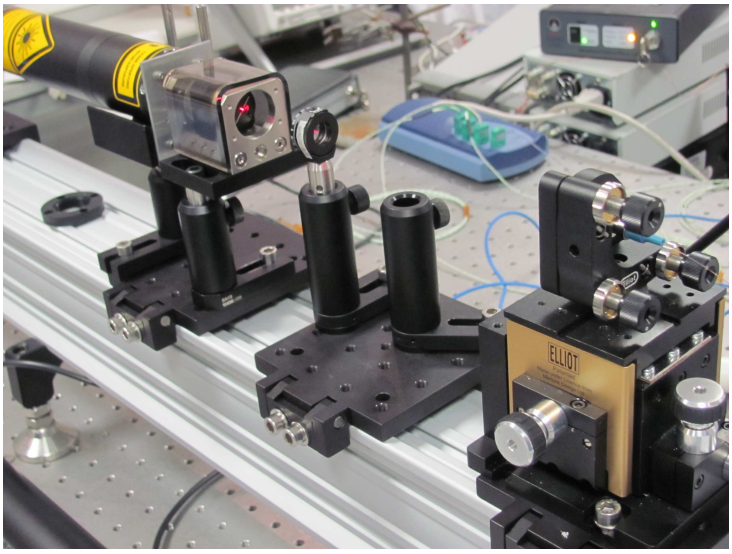

Figure 7: Setup of laser, Faraday isolator, half wave plate, and fiber input.

$$I(\theta) = \frac{1}{2}(S_0 + S_1 \cos^2 2\theta + S_2 \cos 2\theta \sin 2\theta + S_3 sin2\theta) \tag{2.7}$$

where θ is the angle of the quarter wave plate. Using a Fourier analysis and Matlab program, the Stokes parameters can be calculated by rotating the quarter wave plate and taking eight measurements between $0\,^\circ$ and $180\,^\circ$ (every $22.5\,^\circ$). In both cases the degree of polarization P is found in the way described previously.

By measuring the Stokes parameters we hoped to discover the effect that an optical fiber has on the polarization of light. Knowing that we needed a constant polarization at the output, the goal was to achieve that by understanding how the fiber affected the polarization and learn how to achieve a desired polarization at the output.

We decided to use the rotating quarter wave plate model because we had better initial results and were able to calculate uncertainties with our measurements. Our first attempt at measuring the polarization at the input and output of a 800 nm SM 30 m length fiber failed because we used a mislabeled quarter wave plate that was actually a half wave plate. After we fixed this problem, we were able to measure the Stokes parameters on either end of the fiber. We also added a calculation for uncertainties into the

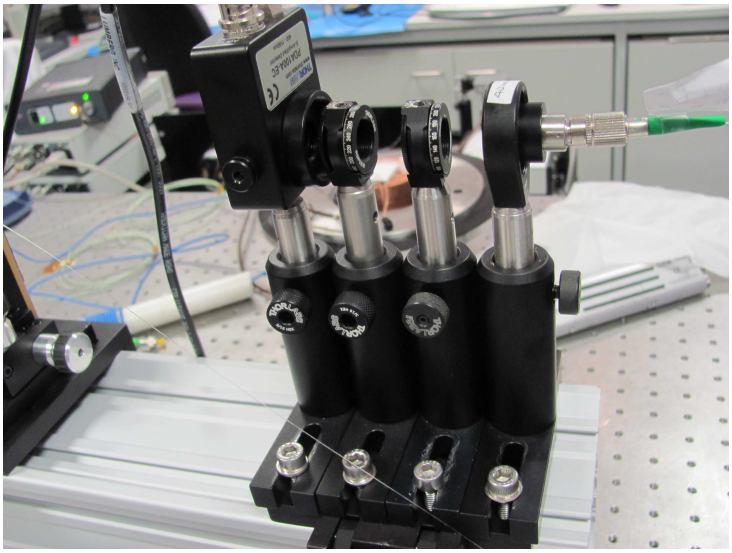

Figure 8: Setup of rotating quarter wave plate method. From right to left: fiber output, rotating quarter wave plate, fixed horizontal polarizer, photo diode.

Matlab program to know how valid our results were.

We also tried controlling the output polarization by using a three paddle polarization controller. The theory is that by wrapping the fiber around each paddle a specified number of times, the first paddle acts as a quarter wave plate to produce linearly polarized light, the second paddle acts as a half wave plate to rotate the polarization, and the third paddle acts as a quarter wave plate to produce the desired output polarization. During the testing and measurements using the polarization controller, we noticed that the intensity reading was not very stable and tended to vary throughout the measurement process. We also noted that the results were not easily repeatable. We attributed this to small fluctuations in the alignment of the beam going into the fiber, which can be caused by the stability of the laser's alignment. Multiple modes would be able to enter the fiber and alter the polarization and intensity because the fiber is specified for 800 nm, not the 633 nm laser we are using. We confirmed this by slightly touching the laser and recording a change in the output polarization. We tried moving the laser closer to the fiber input to cut down on the alignment problem, but we were

unable to achieve stability. By switching to a 633 nm fiber, we were able to limit the transmission to one mode, but we were unable to use the controller because the fiber had a jacket that was too large to fit in the paddles.

3 Examining the Stability of Fiber Optics

As a possible solution to the polarization stability problem, we decided to try using a polarization maintaining (PM) fiber. We tried to measure the Stokes parameters using the rotating quarter wave plate method, but found that the intensity on the output varied too much, which is caused by a change in polarization. This was very frustrating because we thought that the polarization should be maintained at the output. We also tried using a bowtie PM fiber to achieve stability but failed.

After researching the topic, we found that the polarization of the input light needs to be precisely aligned along one of the PM fiber's birefringent axes to maintain the polarization [10]. If it is not aligned, the fiber will be sensitive to environmental disturbances, such as changes in temperature and slight movements of the fiber. These reports matched our experimental findings. To locate the birefringent axes of the fiber, we varied the input polarization by increments of $10\,^\circ$ with a half wave plate and observed the output stability. We first used a 30 m length of 633 nm bowtie PM fiber and found two stability zones with the half wave plate set between $20 - 25\,^\circ$ and $65 - 70\,^\circ$. We then went back and further tested the stability zones (see Table 1 and Table 2) to find the most stable point. After locating $23\,^\circ$ and $66\,^\circ$ as the most stable points, we tested the stability by bending and looping the fiber and observed fluctuations of 10-15 mV compared to variations of up to 100 mV when the fiber is not aligned. It is also important to note that the two stability zones are about $90\,^\circ$ apart (a rotation of θ of the half wave plate produces a 2θ rotation of polarization, so a rotation of the half wave plate by $45\,^\circ$ produces a change of $90\,^\circ$), which fits the prediction that there are two axes that are the most stable.

After achieving a stable polarization, we wanted to measure the Stokes parameters at the output of the fiber using the rotating quarter wave plate method. The results are shown for both stability zones in Table 3 and Table 4. Unfortunately, even though the polarization was much more stable than before, only a small amount of light was recorded at the output, meaning the errors were very large. We could see the light leaking out of the fiber, and

since the fiber was 30 m long, the attenuation of the light was very large. To gain confidence in the stability of the polarization, we placed a polarizer at the output that was crossed with the input polarization. If the polarization was constant, the output light should also be crossed with the polarizer and therefore not pass through it even if bends or loops are made in the fiber. The results of these stability tests are shown in Table 5, Table 6, and Table 7. Even though we found the polarization to be stable, there is too little light to be useful in the interferometer.

To decrease the intensity losses in the fiber, we decided to use a shorter, 1 m length of PM fiber. First, we tried using a 1 m PANDA PM fiber with FC/PC connectors at both ends. Once the connection was optimized, the intensity of the light at the output of the fiber was 9 V, compared to the 1 V we were getting with the 30 m bowtie fiber. The voltage reading, however, varied by hundreds of mV, which is roughly a few percent of the total intensity. Although we were able to get more light at the output of the shorter fiber, we still encountered the same percentage of variability, which we attributed to changes in polarization. We also tried using a 1 m bowtie PM fiber with a FC/PC connectors at one end and FC/APC at the other and a 1 m bowtie PM fiber with FC/PC connectors at both ends. When we used the angled FC/APC connector at the input, we were only able to get 0.7 V of light through, but when we put the FC/APC at the output, we got up to 6 V with variations of 0.7 V.

Rotation Angle of Half Wave Plate ($^\circ$)	Output Variation Range (V)
62	0.315-0.333
64	0.315-0.331
66	0.293-0.301
68	0.308-0.321
70	0.308-0.321
72	0.316-0.325
74	0.282-0.310

Table 1: Stability Zone of 633 nm PM Fiber

Rotation Angle of Half Wave Plate (°)	Output Variation Range (V)
16	0.105-0.146
18	0.098-0.138
20	0.125-0.137
22	0.113-0.118
24	0.113-0.119
26	0.117-0.132
28	0.103-0.118

Table 2: Stability Zone of 633 nm PM Fiber

S_0	0.269 ± 0.074
S_1	0.89 ± 0.540
S_2	0.818 ± 0.540
S_3	-0.135 ± 0.150
DOP	1.22 ± 0.632

Table 3: Stokes Parameters with Half Wave Plate set to 66°

S_0	0.267 ± 0.074
S_1	-0.794 ± 0.540
S_2	-0.674 ± 0.540
S_3	-0.128 ± 0.150
DOP	1.05 ± 0.614

Table 4: Stokes Parameters with Half Wave Plate set to 23°

	$\frac{\lambda}{2}$ plate at 66°, Polarizer at 52°	$\frac{\lambda}{2}$ plate at 24°, Polarizer at 144°
Non-Polarized Intensity (V)	1.12	0.096
Polarized Intensity (V)	0.101	0.098
Intensity Variation with Bend at Input (V)	0.002	0.002
Intensity Variation with Bend at Output (V)	0.002	0.002

Table 5: Stability Test When Bending Fiber

	$\frac{\lambda}{2}$ plate at 66°, Polarizer at 52°		$\frac{\lambda}{2}$ plate at 24°, Polarizer at 144°	
	Without Loops	With Loops	Without Loops	With Loops
Non-polarized intensity (V)	1.11	1.12	1.08	1.08
Polarized Intensity (V)	0.098	0.102	0.098	0.101

Table 6: Stability Test With 10 Loops Around a 25 *mm* Diameter Cylinder Near Output

	$\frac{\lambda}{2}$ plate at 66°, Polarizer at 52°		$\frac{\lambda}{2}$ plate at 24°, Polarizer at 144°	
	Without Loops	With Loops	Without Loops	With Loops
Non-polarized intensity (V)	1.13	1.14	1.10	1.10
Polarized Intensity (V)	0.098	0.125-0.145	0.098	0.125-0.140

Table 7: Stability Test With 5 Loops Around a 40 *mm* Diameter Cylinder Near Output

4 Implementing Fiber Optics with the ILIAD Interferometer

One set of data was taken on June 9th that met the required sensitivity with a 1 m PM patch cable with FC/PC connectors on both ends. The key feature is where the frequency is $10^{-2}Hz$. Here, the angular displacement is about $10^{-9.8}Rad/\sqrt{Hz}$. The required sensitivity of the experiment is at least $8 \times 10^{-10}Rad/\sqrt{Hz}$. Subsequent measurements tired to achieve the same sensitivity, and although we have been close multiple times, we have not yet been able to reproduced the results.

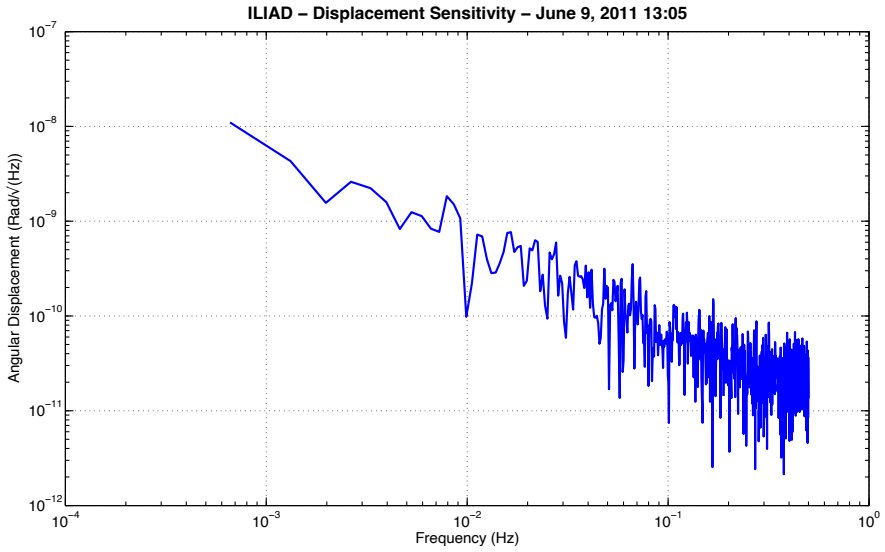

Figure 9: Data taken with 1 m PM patch cable. This was our goal sensitivity.

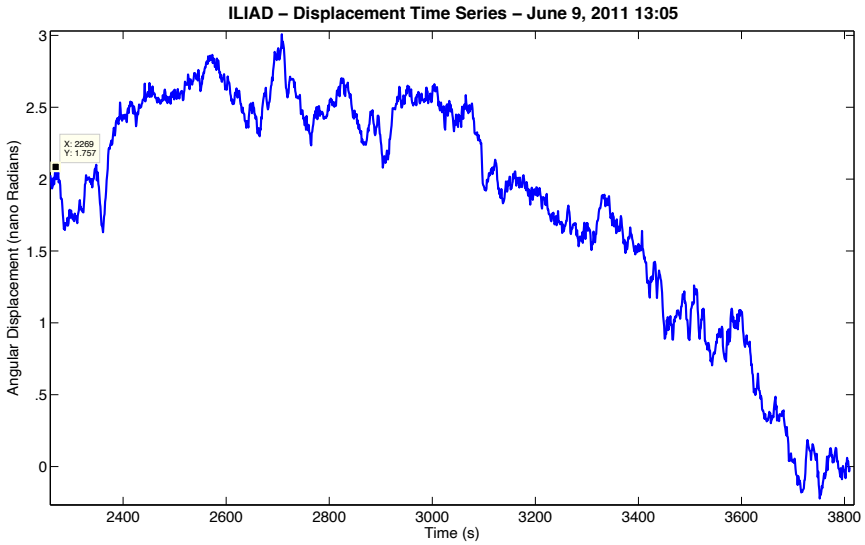

Figure 10: Data taken with 1 m PM patch cable. Varies by only a few nanoradians over the entire data set.

Once we knew how to achieve a constant polarization through the fiber and performed the stability experiments described previously, we began taking data with the ILIAD interferometer with different fibers to try to reach the required sensitivity. We first tried using the 30 m PM fiber with the polarization aligned to the axis. We encountered the same optical loss problem as when we tried to measure the Stokes parameters with this fiber. As a result of the low amount of light, we were not able to achieve as high of sensitivity as we hoped because of digitization errors in the fringe processing software. We switched the laser to frequency stabilized to see if we could get better results but only saw small improvements.

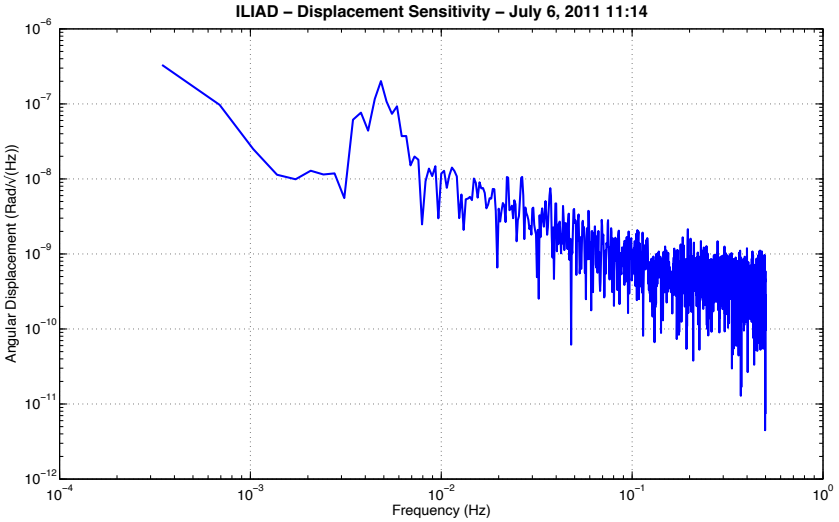

Figure 11: Data taken with 30 m PM bowtie fiber. Laser on intensity stabilized mode.

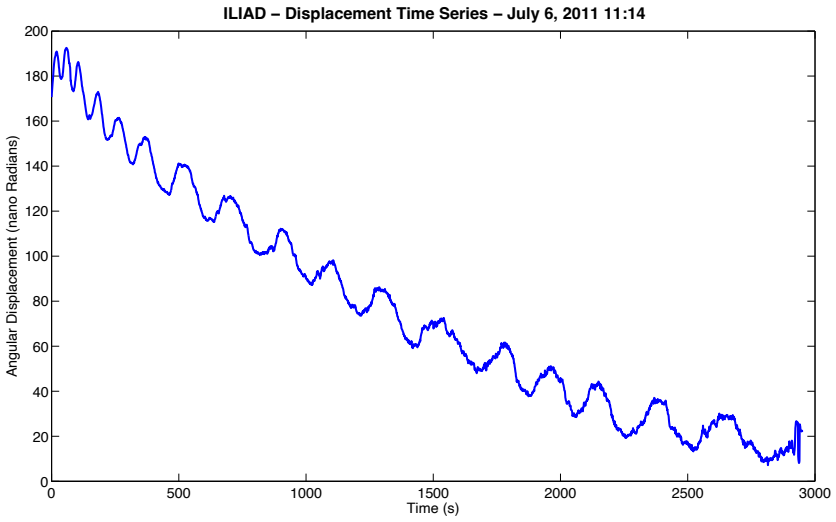

Figure 12: Time series of data taken with 30 m PM bowtie fiber and laser on intensity stabilized mode. Note the oscillations.

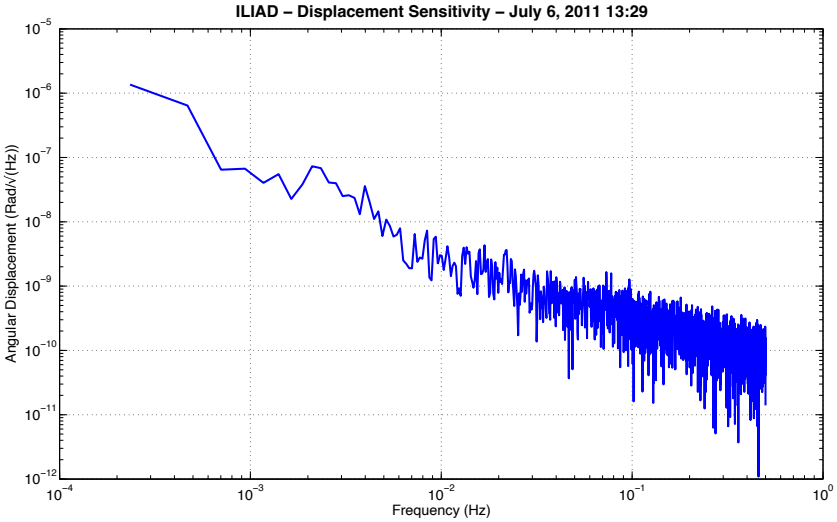

Figure 13: Data taken with 30 m PM bowtie fiber. Laser on frequency stabilized mode.

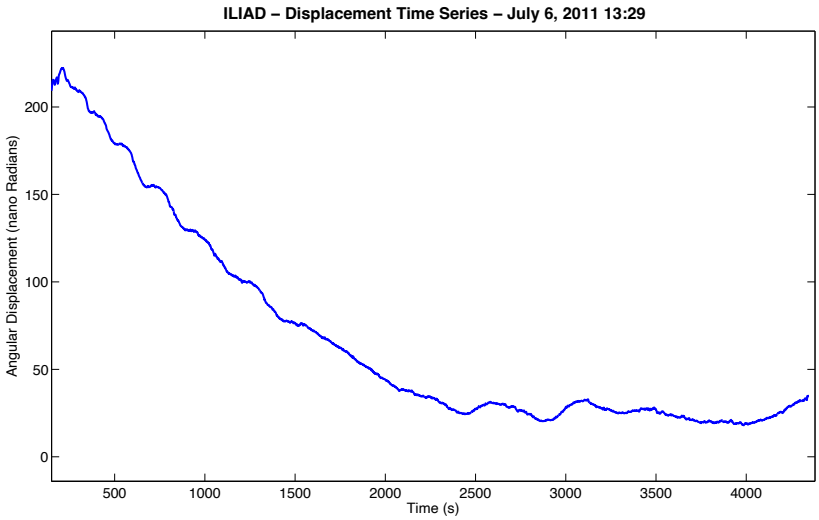

Figure 14: Time series of data taken with 30 m PM bowtie fiber and laser on frequency stabilized mode.

We attempted to decrease the optical loss along the fiber by using a shorter length of fiber. When we connected the 1 m patch cable with FC/PC connectors at both ends to the ILIAD interferometer, we noticed a noise source that caused the interferometer output to oscillated with amplitude of 30 $nrad$. While it was at least a steady oscillation, it was too large to obtain the needed sensitivity. Assuming it was caused by changes in the polarization, we tried bending the fiber and rotating the input polarization to see if either had an effect but neither one did. We also tried switching the laser to both frequency and intensity stabilized modes but did not observe any change. The unknown noise source seemed to be a beat inside the fiber. The next day, we noticed a stray reflection on the fiber input mount. We observed that the reflection oscillated between bright and dark, showing a similar behavior to the oscillations we saw the previous night. When we disconnected the input side of the fiber, the spot disappeared, but when we disconnected the output side from the ILIAD, it remained. After realigning the fiber input to maximize the light through the fiber, we were able to reduce the oscillations to a few nanometers and recorded the data overnight (Figure 15- 18).

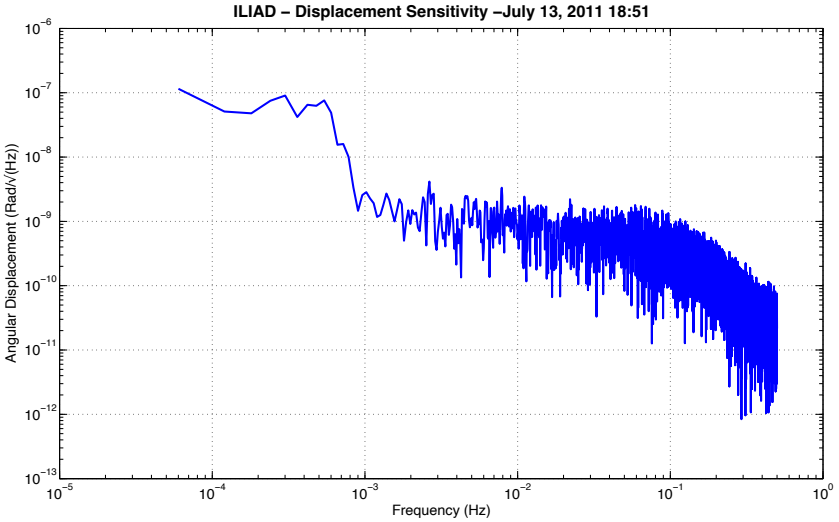

Figure 15: Data taken with 1 m PM bowtie fiber. FC/PC connector at both ends. Laser on intensity stabilized mode. Data taken overnight.

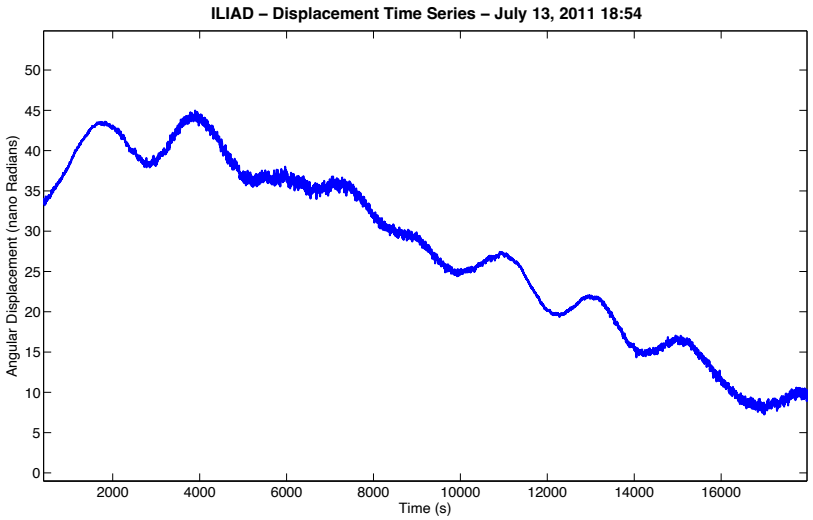

Figure 16: Time series of data taken with 1 m PM bowtie fiber. FC/PC connector at both ends. Laser on intensity stabilized mode. Data taken overnight.

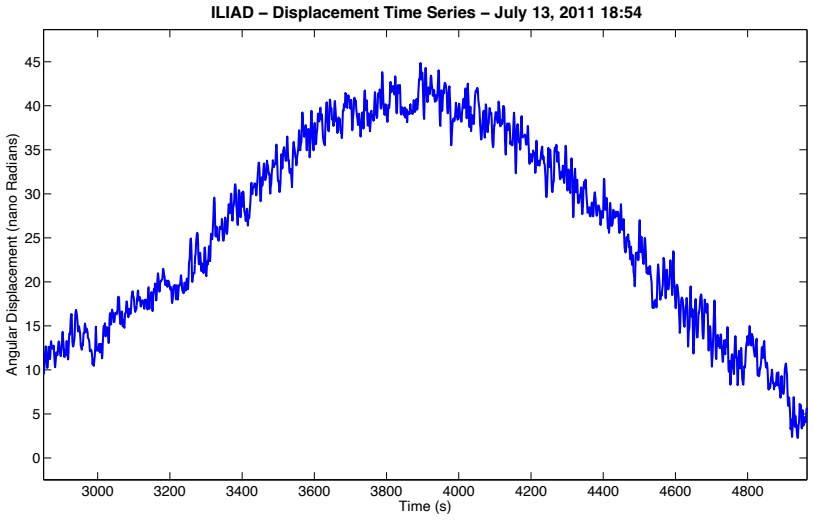

Figure 17: Enlargement of the time series in Figure 16

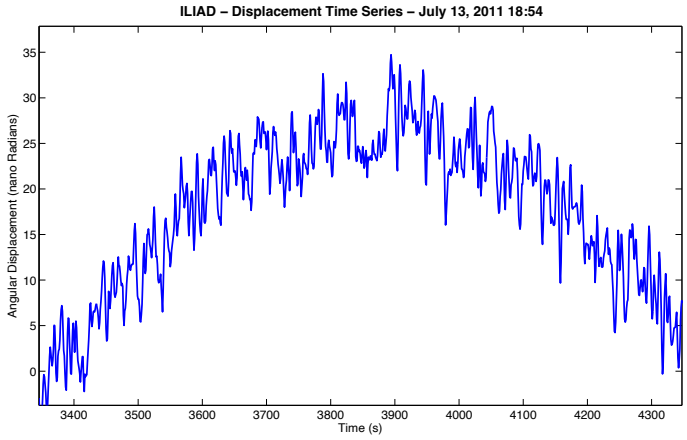

Figure 18: Further enlargement of the time series in Figure 16

After researching the topic the next day, we hypothesized that both the oscillations we observed were caused by Fresnel reflection, also known as back reflection or optical return loss. Fresnel reflection occurs when the refractive index of the fiber is different than that of air causing a percentage of the light to be reflected back into the fiber. When changing from one medium to air, the reflection can be calculated as

$$R = \left(\frac{n-1}{n+1}\right)^2 \tag{4.1}$$

where n is the refractive index. For glass, R is calculated to be 4%. The reflected light could cause the beating interference pattern we observed and explain the oscillating spot's existence. To combat the problem, it is possible to use an index matching material. While the index matching gel would work in the lab setting, we cannot use it during the actual experiment because it would not work when the experiment is cooled down to 4 Kelvin.

As an alternative, we placed the FC/PC connector at the input and the FC/APC at the output to try to reduce any reflections. We identified the polarization stability zones to be when the half wave plate is set to $254-258\,^\circ$ and $300-304\,^\circ$. The results from the first test are shown in Figure 19 and Figure 20. We repeated the measurements to check for repeatability (shown in Figures 21-23).

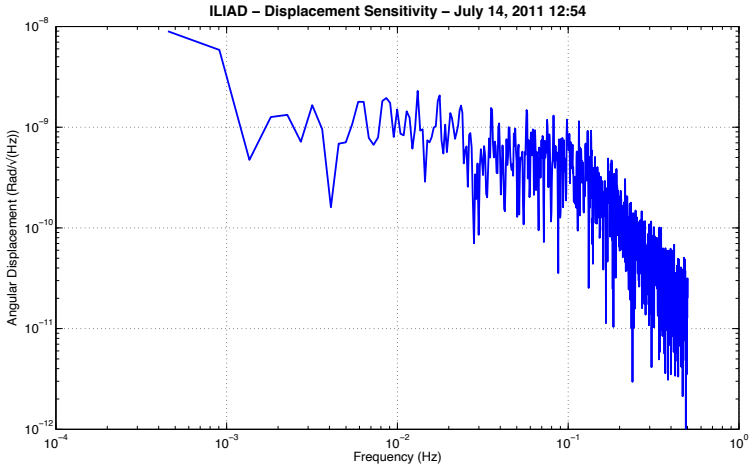

Figure 19: Data taken with 1 m PM bowtie fiber. FC/PC connector at input and FC/APC connector at output. Laser on frequency stabilized mode.

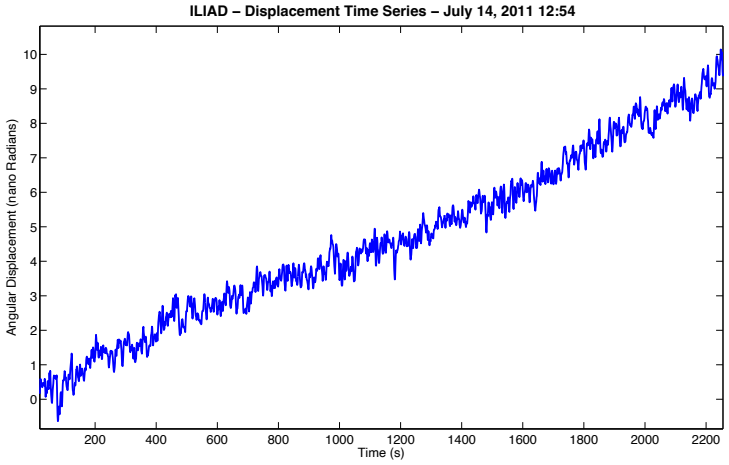

Figure 20: Time series of data taken with 1 m PM bowtie fiber. FC/PC connector at input and FC/APC connector at output. Laser on frequency stabilized mode.

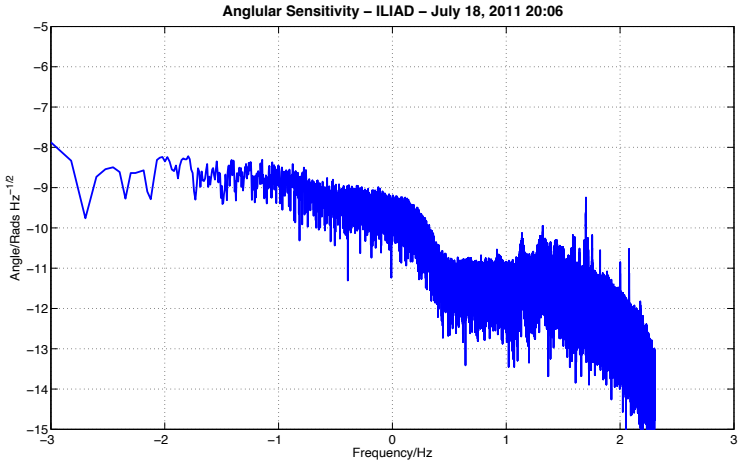

Figure 21: Data taken with 1 m PM bowtie fiber. FC/PC connector at input and FC/APC connector at output. Laser on frequency stabilized mode. Data taken overnight.

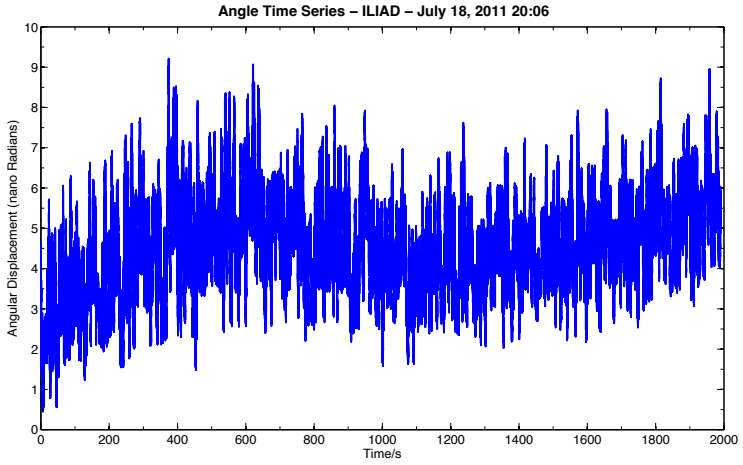

Figure 22: Time series of data taken with 1 m PM bowtie fiber. FC/PC connector at input and FC/APC connector at output. Laser on frequency stabilized mode. Data taken overnight.

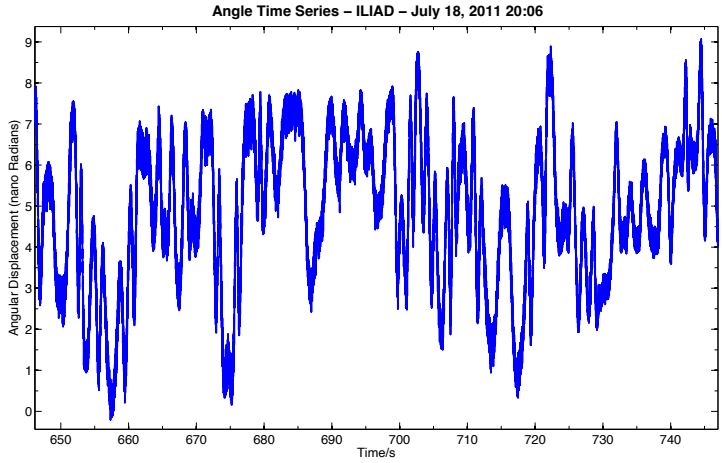

Figure 23: Enlargement of time series in Figure 22

We also tried using a 5 m PM PANDA patch cable with FC/APC connectors at both ends to further reduce the optical feedback but did not get any better results.

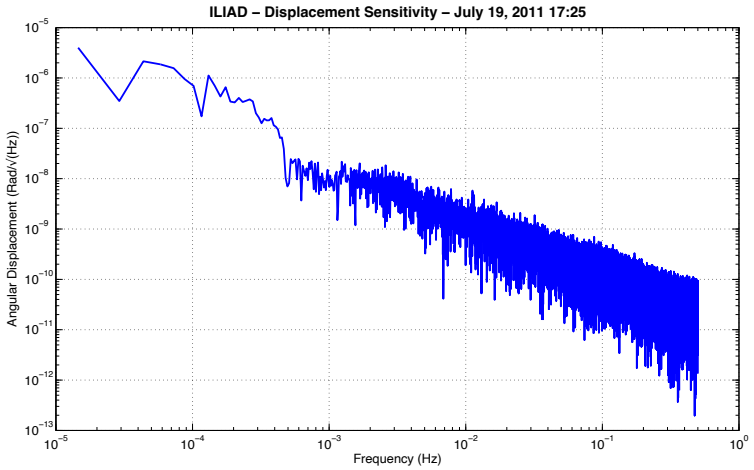

Figure 24: Data taken with 5 m PM PANDA patch cable. FC/APC connectors at both ends.

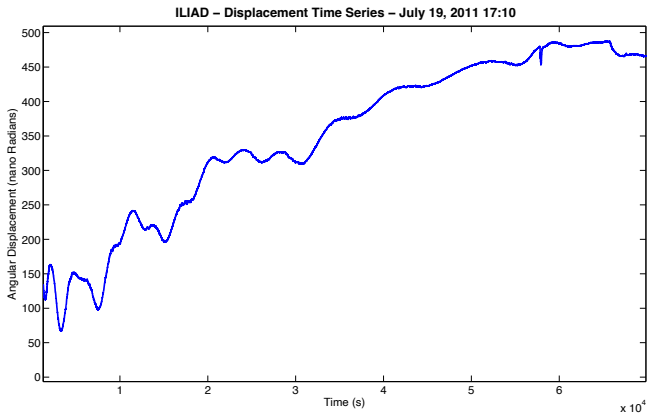

Figure 25: Time series of data taken with 5 m PM PANDA patch cable. FC/APC connectors at both ends.

Date	Fiber Type	Laser Stability	Angular Displacement at $10^{-2}Hz$ $(Rad/\sqrt{Hz})$	Lissajou Pattern Max (V)
June 9	1 m FC/PC PM patch cable		10^{-10}	
July 6 11:14	30 m FC/PC PM bowtie	Intensity	10^{-8}	.703
July 6 13:29	30 m FC/PC PM bowtie	Frequency	$10^{-8.8}$	.675
July 13	1 m FC/PC PM bowtie	Intensity	10^{-9}	
July 14	1 m FC/PC FC/APC PM bowtie	Frequency	10^{-9}	1.76
July 18 20:06	1 m FC/PC FC/APC PM bowtie	Frequency	$10^{-8.5}$	1.87

Table 8: Results from the ILIAD interferometer with different fiber feeds.

4.1 Choosing the Optimal Collimator or Fiberport

To improve our results, we researched using a fiberport that attaches the fiber directly onto the laser head instead of using the collimators we used previously. Thorlabs recommended that we use the fiberports to improve the amount of light transmitted through the fiber and the stability of the setup. The fiberport should theoretically transmit more light because the focal length of the lens it uses better matches our setup than any of the available collimators. To calculate the optimal focal length lens, we used the equation

$$f = \frac{dD\pi}{4\lambda} \tag{4.2}$$

where f is the focal length of the lens, d is the spot diameter of the focal plane (which is the mode field diameter of the fiber), D is the input beam $\frac{1}{e^2}$ diameter, and λ is the wavelength. For our setup with $d = 4.5\ \mu m$, $D = .7$ mm, and λ =633 nm, the calculated focal length is 3.9 mm. The collimators we were using had a focal length of 18.24 mm while the fiberport has a focal length of 2.0 mm. The closest available FC/APC collimator to what we need has a focal length of 7.93 mm, so the fiberport option seems better. We could also purchase a fiberport with a focal length of 4.6 mm which would closely match our system. Attempts at aligning the original fiberport, however, were unsuccessful because it caused the laser to be unstable due to optical feedback. If a collimator was used instead of the fiberport, a Faraday isolator could be used to reduce the optical feedback.

5 Conclusion and Future Work

Despite our better understanding of the polarization of light and how it changes as the light passes through an optical fiber, and our ability to obtain a stable polarization, we were unable to reach the needed sensitivity for the ILIAD interferometer. We used multiple fiber lengths, types, and connectors to try to obtain the needed sensitivity but were unable to achieve easily repeatable results. Furthermore, we encountered a significant amount of Fresnel reflection and optical feedback into the laser which made the system unstable. Multiple attempts to eliminate the feedback problem have been unsuccessful.

Future work includes determining how to prevent optical feedback if a fiberport is used at the head of the laser. If a collimator is used instead optical feedback must still be reduced. Future upgrades to the measurement electronics will allow the user to increase the signal gain and allow less light to be used in the interferometer. With less light, optical feedback would decrease and make the laser more stable. The fiber must also be installed in the experimental housing, which includes using fiber splicing techniques to splice small lengths of copper fiber to PM fibers. The copper fiber is needed at the vacuum connections to prevent leaks, and the PM fiber is used to preserve the polarization. There is also a possibility of adding a fiber polarizer at the end of the spliced fiber to better stabilize the input polarization into the interferometer.

References

[1] N. Arkani-Hamed et al. The hierarchy problem and new dimensions at a millimeter. *Phys Lett*, B429(3-4):263–272, 1998.

[2] C. C. Speake et al. Documentation for STFC Oversight committee. Technical report, University of Birmingham, 2011.

[3] B. Schaefer et al. Measuring the Stokes polarization parameters. *Am. J. Phys*, 75(2):163–168, February 2007.

[4] E. Collett. *Field Guide to Polarization*. SPIE Publications, 2005.

[5] M. P. Varnham et al. Bend behaviors of polarizing optical fibers. *ELECTRON LETT*, 19(17):679–680, August 1993.

[6] M. P. Varnham et al. Coiled-birefringent-fiber polarizaers. *OPT LETT*, 9(7):306–308, July 1984.

[7] Fiber cable types. `http://www.audiorail.com/fiber_converters.htm`.

[8] Polarization maintaining fibers. `http://www.audiorail.com/fiber_converters.htm`.

[9] E. Collett. Measurement of the four Stokes polarization parameters with a single circular polarizer. *OPT COMMUN*, 52(2):77–80, November 1984.

[10] E. Collett. *Polarized Light in Fiber Optics*. SPIE Press, 2003.